ISSN 1027-5495. Functional Materials, 28, No.3 (2021), p. 427-436.
doi:https://doi.org/10.15407/fm28.03.427

Dielectric and magnetic properties of $KTaO_3$ co-doped with Li and Co: size effects

***S.V.Lemishko*[1], *O.O.Andriiko*[2], *M.M.Prokopiv*[3], *M.O.Tripachko*[4], *I.S.Golovina*[1,5]**

[1]V.Lashkaryov Institute of Semiconductor Physics, National Academy of Sciences of Ukraine, 41 Nauky Ave., 03028 Kyiv, Ukraine
[2]National Technical University of Ukraine, "“Igor Sikorsky Kyiv Polytechnic Institute”", 37 Peremogy Ave., 03056 Kyiv,Ukraine
[3]V.Bakul Institute for Superhard Materials, National Academy of Sciences of Ukraine, 2 Avtozavodska Str., 04074 Kyiv, Ukraine
[4]Institute of Physics, National Academy of Sciences of Ukraine, 46 Nauky Ave., 03020 Kyiv,Ukraine
[5]Drexel University, 3141 Chestnut Str., Philadelphia, 19104 PA, USA

Received September 22, 2021

We present dielectric and magnetic properties of potassium tantalate $KTaO_3$ co-doped with Li (4 mol.%) and Co(4 mol. %) for different powder particle sizes: 200 nm (submicron crystals) and 80 nm (nanosized crystals). As-synthesized submicron crystals have a cubic shape with rounded corners, while nanosized crystals have an elongated parallelepiped shape with clear even edges. The dielectric relaxation parameters of Li atoms are determined using the Vogel-Fulcher law: activation energy E_a = 0.0167 eV and characteristic frequency $\nu_0 = 10^7$ Hz. A significant decrease in these parameters was found in comparison with $KTaO_3$ doped only with lithium, which indicates the role of cobalt in the dynamics of off-center lithium atoms. The kinetic parameters describing the relaxation behavior of Co atoms are also determined. The parameters are found to be very close: E_a = 0.387±0.05 eV, $\nu_0 = (2.5\pm0.8)\cdot10^{13}$ Hz and E_a =0.391±0.05 eV, $\nu_0 = (3\pm1)\cdot10^{13}$ Hz for a submicron and nanosized sample,respectively. The formation of cluster magnetism with the presence of clusters of different sizes is established. As the temperature changes from 110 to 290 K,the average size of clusters increases from 2115 to 3360 and from 3071 to 5577 Co atoms per cluster for a submicron and nanosized sample, respectively.

Keywords: potassium tantalate, size effect, relaxor ferroelectric, dielectric relaxation, cluster magnetism.

Діелектричні та магнітні властивості $KTaO_3$, легованого Li і Co: розмірні ефекти. *С.В.Лемішко, О.О.Андрійко, М.М.Прокопів, М.О.Трипачко, І.С.Головіна*

Представлено діелектричні та магнітні властивості танталату калію $KTaO_3$, легованого одночасно Li (4 мол.%) та Co (4 мол.%), для різних розмірів частинок вихідних порошків, 200 нм (субмікронні кристали) та 80 нм (нанорозмірні кристали). Синтезовані субмікронні кристали мають кубічну форму з округлими кутами, в той час як нанорозмірні кристали мають продовгувату форму паралелепіпеда з чіткими рівними ребрами. Із використанням закону Фогеля-Фулчера встановлено параметри діелектричної релаксації атомів Li: енергія активації E_a = 0.0167 еВ і характеристична частота $\nu_0 = 10^7$ Гц. Виявлено значне зменшення значень даних параметрів порівняно із $KTaO_3$, легованим тільки Li, що вказує на роль кобальту у динаміці нецентральних атомів літію. Також встановлено кінетичні параметри, які описують релаксаційну

поведінку атомів Co. Параметри практично однакові: $E_a = 0.387 \pm 0.05$ еВ, $\nu_0 = (2.5 \pm 0.8) \cdot 10^{13}$ Гц і $E_a = 0.391 \pm 0.05$ еВ, $\nu_0 = (3 \pm 1) \cdot 10^{13}$ Гц для субмікронного и нанорозмірного зразка відповідно. Встановлено формування кластерного магнетизму з наявністю кластерів різного розміру. При зміні температури від 110 до 290 K середній розмір кластерів зростає від 2115 до 3360 та від 3071 до 5577 атомів Co на один кластер для субмікронного та нанорозмірного зразка відповідно.

Представлены диэлектрические и магнитные свойства танталата калия $KTaO_3$, легированного одновременно Li (4 мол%) и Co (4 мол%) для различных размеров частиц исходных порошков, 200 нм (субмикронные кристаллы) и 80 нм (наноразмерные кристаллы). Синтезированные субмикронные кристаллы имеют кубическую форму с закругленными углами, в то время как наноразмерные кристаллы имеют удлиненную форму параллелепипеда с четкими ровными краями. Параметры диэлектрической релаксации атомов Li определяются с использованием закона Фогеля-Фулчера: энергия активации $E_a = 0.0167$ эВ и характеристическая частота $\nu_0 = 10^7$ Гц. Обнаружено значительное уменьшение значений данных параметров по сравнению с $KTaO_3$, легированным только Li, что указывает на роль кобальта в динамике нецентральных атомов лития. Определены кинетические параметры, описывающие релаксационное поведение атомов Co. Параметры практически идентичны: $E_a = 0.387 \pm 0.05$ эВ, $\nu_0 = (2.5 \pm 0.8) \cdot 10^{13}$ Гц и $E_a = 0.391 \pm 0.05$ эВ, $\nu_0 = (3 \pm 1) \cdot 10^{13}$ Гц для субмикронного и наноразмерного образца соответственно. Установлено образование кластерного магнетизма с наличием кластеров разных размеров. При изменении температуры от 110 до 290 K средний размер кластеров увеличивается от 2115 до 3360 и от 3071 до 5577 атомов Co на кластер для субмикронного и наноразмерного образца соответственно.

1. Introduction

Potassium tantalate ($KTaO_3$, KTO) is an incipient ferroelectric, which is often used as a model structure in fundamental studies of the physics of ferroelectrics [1, 2]. From application standpoint, this material is of interest due to its low dielectric loss ($\tan\delta = 10^{-4}$) and high dielectric constant, which grows monotonically from 261 at 300 K to 4000 at 4.2 K without frequency dependence, and therefore, it is used as a dielectric microwave resonator to increase the sensitivity of radiospectroscopic research methods [3–7]. Factors that can affect material properties are used to expand the scope of applications. The most popular of them are crystal size reduction and doping. The ferroelectric phase transition and magnetic properties were detected in nanoscale crystals of $KTaO_3$, which are caused by defects [8–10] such as uncontrolled iron impurity, and oxygen vacancies, that hybridize in the surface layer of nanoparticles and become magnetic [11]. The use of lithium as dopant changes the properties of potassium tantalate so that it passes into a qualitatively different phase state and changes its structure depending on the Li concentration. Lithium replaces potassium and, due to of the large difference in ionic radii ($r_K = 1.33$ Å, $r_{Li} = 0.69$ Å), shifts from the centrosymmetric position to a distance 1.26 Å along the [100] direction and forms an electric dipole [12–14]. At low concentrations of Li ($0.02 < x < 0.05$), mixed compounds of $K_{1-x}Li_xTaO_3$ have relaxor properties (dipole glass) [15–18]. At concentrations $x > 0.05$, the material becomes a classic ferroelectric [19]. Non-magnetic in the bulk, KTO can also have magnetic properties either upon reduction of crystallites [20], or upon doping, for example, with cobalt [21].

In this work, we apply both approaches: doping of potassium tantalate with lithium and cobalt simultaneously and synthesizing the material using various technologies that make it possible to obtain crystals of different sizes. After developing a technological procedure for the manufacture of ceramic samples, establishing the phase composition, characteristics of microstructure and morphology, we study the dielectric and magnetic properties of the material.

2. Experimental

Ceramic samples were made in two stages: 1) synthesis of powders of corresponding composition and structure; 2) pressing and sintering of the synthesized powders. The powders were synthesized by two methods for obtaining crystals of different sizes. Solid-phase synthesis was used to obtain crystals of a submicron range, while a technology based on oxidation of metallic Ta in the molten KNO_3 [22] was used to obtain nanosized crystals.

2,1. Solid-phase synthesis method

Powders K_2CO_3, Ta_2O_5, Co_3O_4 and Li_2CO_3 were used as starting materials for

the synthesis. The weight fractions of the components were determined according to the reaction equation:

$$K_2CO_3 + Ta_2O_5 + Li_2CO_3 + Co_3O_4 \rightarrow K_{1-x-2y}Li_xCo_yTaO_3 + CO_2\uparrow, \quad (1)$$

where $x = 0.04$ and $y = 0.04$. Extra amount of K_2CO_3 (35 wt. %) was added to compensate for the loss of evaporation of potassium during the synthesis process. After mechanical mixing of the starting components, the mixture was calcinated at a temperature of 800°C for 8 h.

Powders of $KTaO_3$ (KTO) and $K_{0.88}Li_{0.04}Co_{0.04}TaO_3$ (KLCTO I) were synthesized using this method.

2.2. Oxidation of metallic tantalum method

Application of the method of oxidation of metallic Ta in molten KNO_3 for the synthesis of nanocrystalline KTO is described in detail elsewhere [22]. The basic structure of potassium metatantalate is formed in the molten mixture of potassium nitrate and potassium hydroxide at 650°C according to the reaction equation:

$$2KOH + 2Ta + 5KNO_3 \rightarrow 2KTaO_3 + 5KNO_2 + H_2O.$$

To avoid the formation of impurity phases of polytantalates, an excess of potassium hydroxide is required. After cooling the melt, the formed potassium nitrite was washed with water and the product was dried at a temperature of about 100°C. Thereby, pure potassium tantalate was obtained.

To obtain doped potassium tantalate, the ratio of potassium nitrate to tantalum must remain unchanged, and part of the potassium hydroxide must be replaced by the required amount of compounds of the doped element. Potassium tantalate with 4 mol.% lithium and 4 mol.% cobalt was obtained by oxidizing tantalum powder in molten potassium nitrate and introducing doping components in quantities corresponding to the reaction equation with the addition of 20 % excess KOH:

$$1.76KOH + 0.08LiOH + 0.08Co(NO_3)_2 + 2Ta + 5KNO_3 \rightarrow 2K_{0.88}Li_{0.04}Co_{0.04}TaO_3 + 5KNO_2 + 0.92H_2O + 0.16NO_2 + 0.04O_2.$$

The powder $K_{0.88}Li_{0.04}Co_{0.04}TaO_3$ (KLCTO II) was synthesized using this method.

2.3. Producing of ceramic samples

The synthesized powders were pressed into tablets by cold static pressing at a pressure of 300 MPa for 5 min. The sintering temperature was determined by analyzing the temperature dependence of the shrinkage of the test samples. The test samples were pressed and subjected to a slow heating. At some point in the heating process, the samples size starts to decrease, that indicates the beginning of the sintering process. As the temperature increases further, the sample size reaches its minimum size and no longer shrinks, which indicates the completion of the sintering process. The shrinkage termination temperature is optimal for sintering ceramic specimens. Therefore, compressed pellets of pure KTO were sintered at a temperature of 1550 K, and KTO pellets doped with Li and Co were sintered at 1520 K. For all samples, the rate of heating and cooling was 5°/min and the sintering time was 2 h. The obtained ceramic specimens were buffed and polished. To determine the grain size, the samples were subjected to thermal annealing at a temperature 50 K below the sintering temperature for 10 min to clear grain boundaries; then gold was sputtered onto the surface.

The phase composition and structure were investigated by X-ray diffraction (XRD) technique using a diffractometer AXS D8 (Bruker, Germany) with radiation $Mo_{K\alpha 1}$ (wavelength $\lambda = 0.0709$ nm) at room temperature. The crystallite size and morphology were characterized by the scanning electron microscopy (SEM) method using a microscope XL 30 FEG (Philips, Netherlands). The density of ceramic samples was determined by the Archimedes method. For dielectric measurements, the Pt electrodes were sputtered on the plane-parallel surfaces of the samples. The dielectric characteristics (dielectric constant and dielectric loss) were measured using an instrument LCR E7-20 (Belarus) within the temperature range 4.2 K $< T <$ 250 K at frequencies 1 kHz, 10 kHz, 100 kHz and 1 MHz and High Performance Frequency Analyzer Alpha A (Novocontrol, Montabaur, Germany) within the temperature range 150 K $< T <$ 300 K at frequencies 1 Hz, 10 Hz, 100 Hz, 1 kHz, 10 kHz, 100 kHz and 1 MHz. The dielectric properties were studied in the interval from 4.2 K to 250 K for KTO and KLCTO I samples and in the

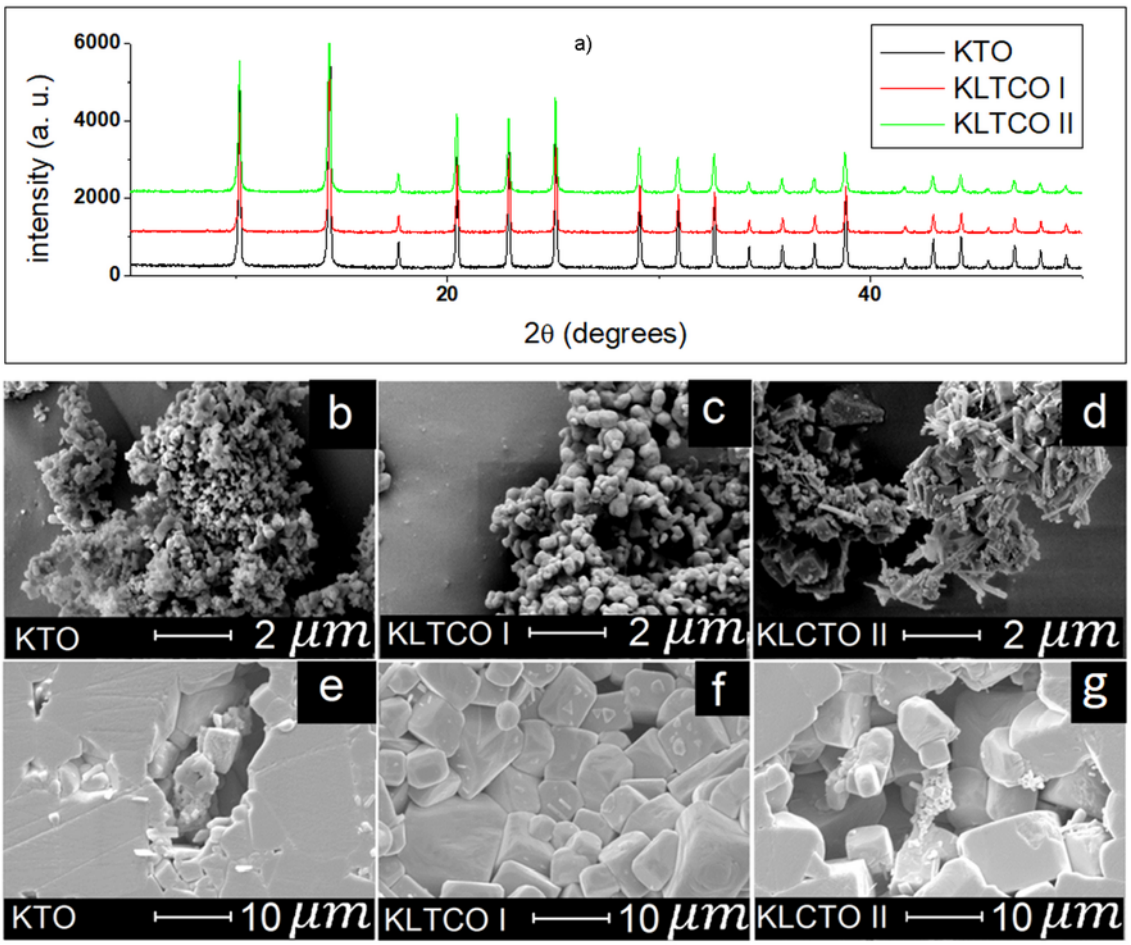

Fig. 1.(a) XRD spectra of undoped and doped potassium tantalate powders. The SEM images of powders: (b) — KTO, (c) — KLCTO I, (d) — KLCTO II (magnification 20000×). The SEM images of ceramic samples: (e) — KTO, (f) — KLCTO I, (g) — KLCTO II (magnification 5000×).

interval from 150 K to 300 K for KLCTO II. The magnetic hysteresis loops were recorded using an instrument LDJ 9500 in applied magnetic fields from −50000 A/m to 50000 A/m at temperatures 110 K 150 K, 200 K, 250 K, and 290 K.

3. Results and discussion

According to the XRD data, as-synthesized powders as well as ceramic samples contain a pure KTO phase. No impurity phases were observed in undoped KTO, doped KLCTO I and KLCTO II samples (Fig. 1a). The peaks in the XRD spectra do not shift upon doping, so the lattice parameters remain unchanged. Consequently, the doped KLTCO I and KLTCO II powders, like the undoped KTO, have cubic symmetry with a parameter a = 3.988 Å at room temperature. A similar result was obtained for ceramic samples.

The SEM images for each of the synthesized powders are shown in Figs. 1b, c, d. According to the SEM data, the average particle size is 120 nm, 200 nm and 80 nm for KTO, KLTCO I and KLTCO II, respectively. A significant difference in the morphology of powder particles obtained by different technologies is revealed. While the KTO and KLTCO I powders have cubic particles with rounded corners, the KLTCO II powder has elongated formations, the longitudinal dimension of which is much larger than the transverse one, and the edges are clear and even.

The SEM images of ceramic samples (Figs. 1e, f, g) show that KTO is characterized by a compacted structure with isolated pores, outside of which the material looks solid. KLCTO I has a granular microstructure with a grain size from 1 to 10 μm. KLCTO II has a high porosity, that is consistent with the low density of the ceramic sample mentioned below. As well,

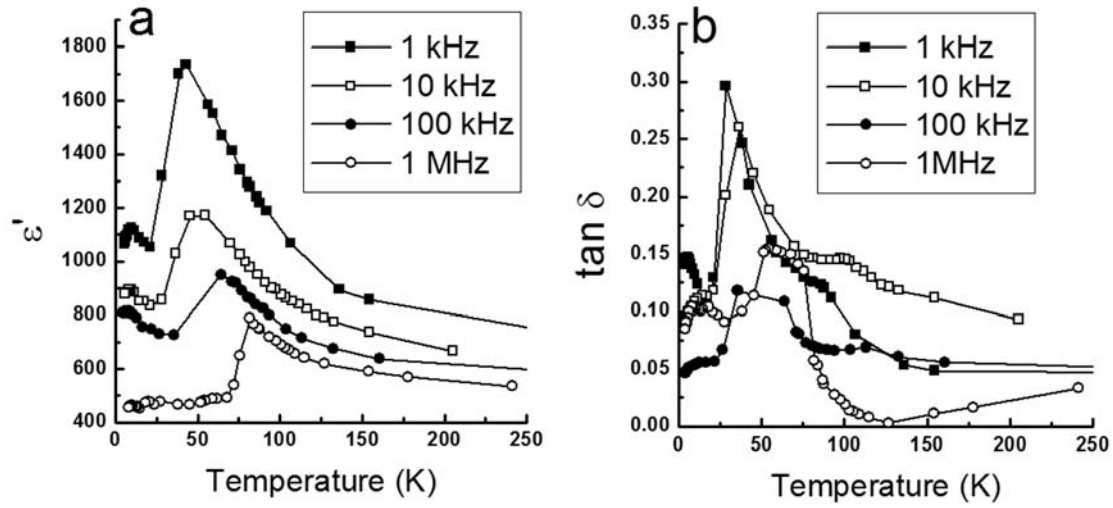

Fig.2. Temperature dependence of dielectric constant (a) and dielectric losses (b) at frequencies 1 kHz, 10 kHz, 100 kHz and 1 MHz for KLCTO I sample.

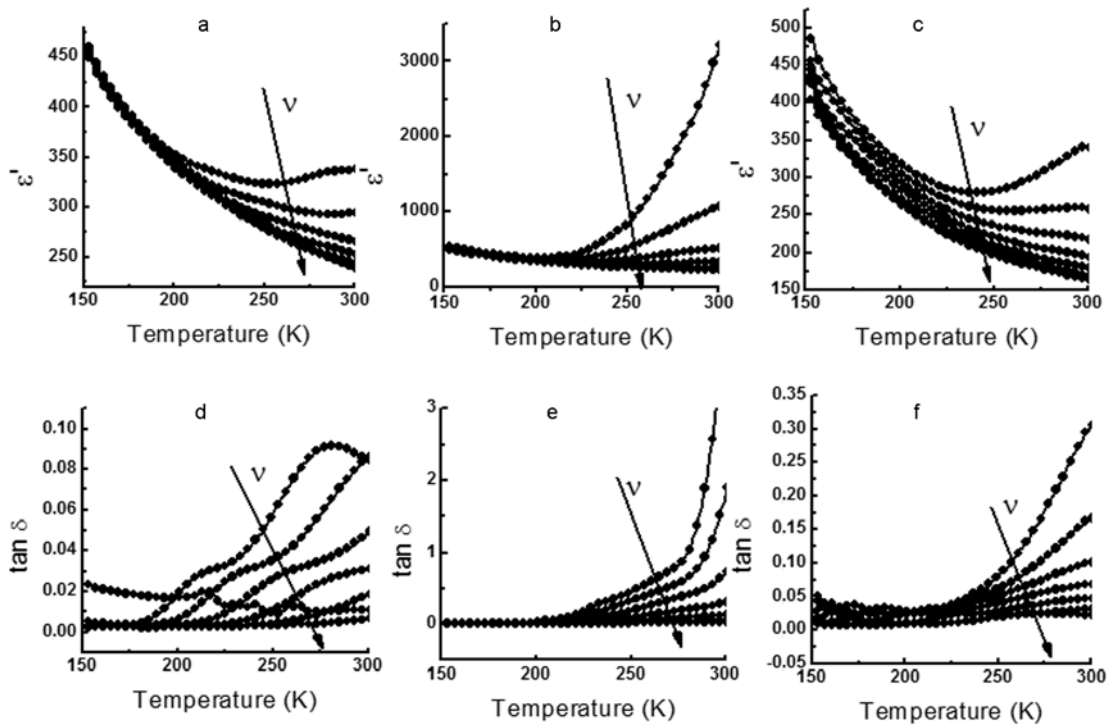

Fig. 3. Temperature dependences of dielectric constant and dielectric losses for KTO (a, d), KLCTO I (b, e) and KLCTO II (c, f) samples at frequencies 1 Hz, 10 Hz, 100 Hz, 1 kHz, 10 kHz, 100 kHz and 1 MHz.

the agglomerations of small grains less than 1 μm in size are observed on the background of larger grains up to 10 microns in size. In addition to a significant increase in the particle size compared to the as-synthesized powder, a change in the morphology of the particles is observed in ceramic KLCTO II sample. The oblong shape of the powder particles (Fig. 1d) transforms into a symmetrical cubic shape in ceramics (Fig. 1g).

The density of the ceramic samples compared to the theoretical density of potassium tantalate is: 81±3.5 % (KTO), 86±6 % (KLCTO I) and 70±1 % (KLCTO II). This density makes it possible to reliably meas-

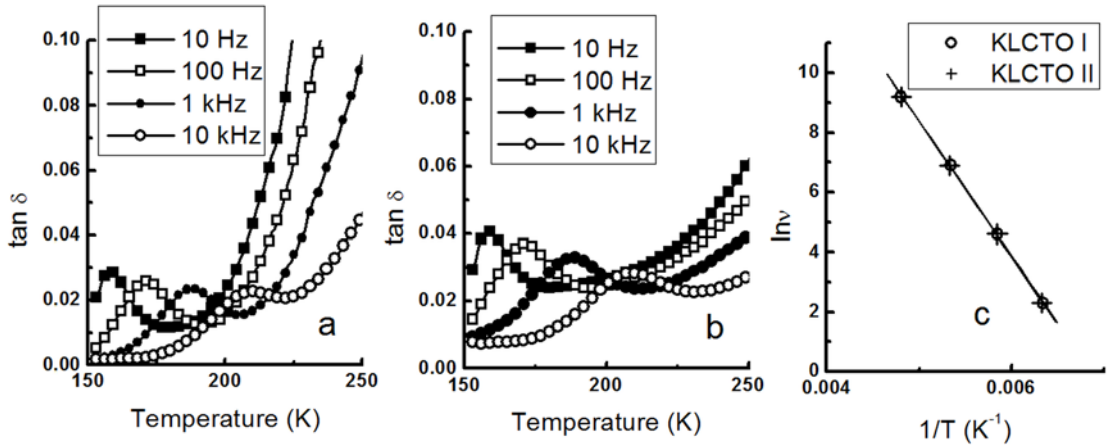

Fig. 4. Temperature dependences of dielectric losses in the range from 150 K to 250 K at different frequencies for the KLTCO I (a) and KLTCO II (b) samples. Arrhenius linearized dependence for KLCTO I and KLCTO II (c).

ure the dielectric properties at temperatures below 250 K. At temperatures above 250 K, dielectric losses can increase due to electrical conductivity caused by the high porosity.

The temperature dependences of dielectric constant (ε′ and dielectric losses (tanδ) for all ceramic samples are presented in Figs. 2 and 3.

A feature observed in many relaxor ferroelectrics and particularly in potassium tantalate doped with lithium, $K_{1-x}Li_xTaO_3$ at $0.02 < x < 0.05$ [15–18], is the dependence on T_{max}, which is the temperature corresponding to the maximum ε′ at the measuring frequency. This dependence has a form of the Vogel-Fulcher law [23]:

$$\nu = \nu_0 e^{-\frac{E_a}{k_B(T_{\max} - T_{VF})}}, \quad (1)$$

where ν is the measuring frequency; ν_0 is the characteristic frequency; E_a is the activation energy, k_B is the Boltzmann constant; T_{max} is the temperature value corresponding to the maximum dielectric constant; T_{VF} is the Vogel-Fulcher temperature. At the Vogel-Fulcher temperature, the dynamics of Li dipoles is frozen.

To determine the values of T_{VF}, E_a and ν_0 parameters, the positions of the maximum ε′(T) at three measuring frequencies are required. Then, the Vogel-Fulcher temperature is determined as:

$$T_{VF} = \frac{T_3 - T_2 \frac{\ln\nu_1 - \ln\nu_2 T_1 - T_3}{\ln\nu_1 - \ln\nu_3 T_1 - T_2}}{1 - \frac{\ln\nu_1 - \ln\nu_2 T_1 - T_3}{\ln\nu_1 - \ln\nu_3 T_1 - T_2}}, \quad (2)$$

activation energy is determined as:

$$E_a = \frac{(\ln\nu_1 - \ln\nu_3)(T_3 - T_{VF})(T_1 - T_{VF})}{T_1 - T_3} k_B, \quad (3)$$

and characteristic frequency is determined as:

$$\nu_0 = \nu_1 e^{\frac{E_a}{k_B(T_1 - T_{VF})}}. \quad (4)$$

Using experimental values $T_1 = 43$ K, $T_2 = 50$ K and $T_3 = 64$ K taken from Fig. 2a at frequencies $\nu_1 = 1$ kHz, $\nu_2 = 10$ kHz and $\nu_3 = 100$ kHz, respectively, and formulas (2)–(4), the parameters T_{VF}, E_a and ν_0 have been calculated. The computed parameters are shown in Table 1. For comparison, the parameters for KTO doped with Li, obtained in [23], are also included in Table 1.

Comparison of the parameters of the Vogel-Fulcher dependence, determined for KLCTO I, with the values obtained by [23] for KLT (4.4 %) indicates a significant effect of cobalt, which results in a decrease in the characteristic frequency of relaxation ν_0 by almost two orders of magnitude and to a decrease in the activation energy E_a by more than 5 times. The above parameters describe the relaxation dynamics of polar nanoclusters formed by Li atoms, which replace K atoms in KTO and occupy the off-central position creating dipole centers. This result can confirm that Co atoms also replace K and therefore significantly affect the relaxation behavior of Li atoms.

Figure 4 shows the dielectric losses (tanδ) within the temperature interval from 150 K to 250 K for KLCTO I and KLCTO II samples. In both samples there is a maxi-

Table 1. Parameters for the Vogel-Fulcher dependence

Parameter	KLCTO I	KLT [23]
T_{VF}, K	22	26.5
E_a, eV	0.0167	0.0856
ν_0, Hz	10^7	$2.81 \cdot 10^9$

mum in tanδ(T) that has a pronounced frequency dependence. The maximum is positioned at $T = 157$ K and 10 Hz. As frequency increases, the maximum shifts to higher temperatures. At this, the intensity of the maximum decreases and the width increases. Such a behavior of the tanδ(T) peak as a function of frequency indicates the presence of a dipole relaxation center and represents its kinetics. In [24] suggest that the maximum of tanδ at $T = 185$ K and 1 kHz corresponds to the relaxation of Co^{2+} ions in KTO doped with cobalt.

It is known that the kinetics of the dipole center with temperature obeys the Arrhenius law [24, 25]:

$$\nu = \nu_0 \exp\left(-\frac{E_a}{k_B T}\right). \quad (5)$$

The notations of parameters in (5) are identical to those in equation (1).

Thus, from the frequency dependence of the position of the maximum, the following kinetic parameters can be determined: activation energy E_a and characteristic frequency ν_0. If the experimental data is obtained at two frequencies, the parameters are calculated as follows. Activation energy is calculated using the formula [26]:

$$E_a = \frac{T_1 T_2 k_B}{T_2 - T_1} \ln\left(\frac{\omega_2}{\omega_1}\right). \quad (6)$$

Here ω_1, ω_2 are the cyclic frequencies for two maxima ($\omega = 2\pi\nu$; T_1, T_2 are corresponding temperatures; k_B is the Boltzmann constant. The relaxation time is determined by the formula:

$$\tau_0^{-1} = 2\pi\nu_1 e^{E_a/k_B T_1}, \quad (7)$$

using the condition $\omega\tau_1=1$ for the maximum [25].

For accurate determination of the relaxation parameters, we use the data collected not at two but at four frequencies, as shown in Fig. 4. The temperatures corresponding to the position of the tanδ(T) maximum taken from Fig. 4 are shown in Table 2. We

Table 2. Position of the tanδ(T) maximum at different frequencies in KLCTO I and KLCTO II

Sample	10 Hz	100 Hz	1 kHz	10 kHz
KLCTO I	157.5 K	171 K	187 K	208 K
KLCTO II	158 K	171 K	187.5 K	208 K

use the method of linearization of the Arrhenius dependence and calculate values from the approximated linear dependence using the least-square deviation method (using all available points at once).

From the Arrhenius equation for the relaxation frequency (5), we obtain the dependence of lnν on the reciprocal temperature as follows:

$$\ln\nu = -\frac{E_a}{k_B} \cdot \frac{1}{T} + \ln\nu_0. \quad (8)$$

This is a linear dependence, $y = Kx + B$, with parameters $K = -E_a/k_B$ and $B = \ln\nu_0$.

The result of linearization of the Arrhenius dependence is presented in Fig. 4c. It can be seen that the experimental data are well described by the lnν($1/T$) dependence. The parameters for the approximation line are calculated as follows:

$$K = \frac{n\sum\left(\ln\nu \cdot \frac{1}{T}\right) - \sum\frac{1}{T}\sum\ln\nu}{n\sum\left(\frac{1}{T}\right)^2 - \left(\sum\frac{1}{T}\right)^2} \quad (9)$$

$$B = \frac{\sum\ln\nu - K\sum\frac{1}{T}}{n}. \quad (10)$$

Using the K and B values, we find the parameters of the Arrhenius equation as follows:

$$\nu_0 = e^B, \quad E_a = -Kk_B. \quad (11)$$

Applying the described approach and the method of linearization of the Arrhenius dependence, the values of relaxation parameters were determined: activation energies $E_a = 0.387 \pm 0.05$ eV and $E_a = 0.391 \pm 0.05$ eV and characteristic frequencies $\nu_0 = (2.5 \pm 0.8) \cdot 10^{13}$ Hz and $\nu_0 = (3 \pm 1) \cdot 10^{13}$ Hz for KLCTO I and KLCTO II, respectively. As we can see, the relaxation parameters are almost identical for both samples. These values are very close to the values obtained in [24] for Co^{2+} dipole centers in KTO doped with cobalt: $E_a = 0.36$ eV, $\nu_0 =$

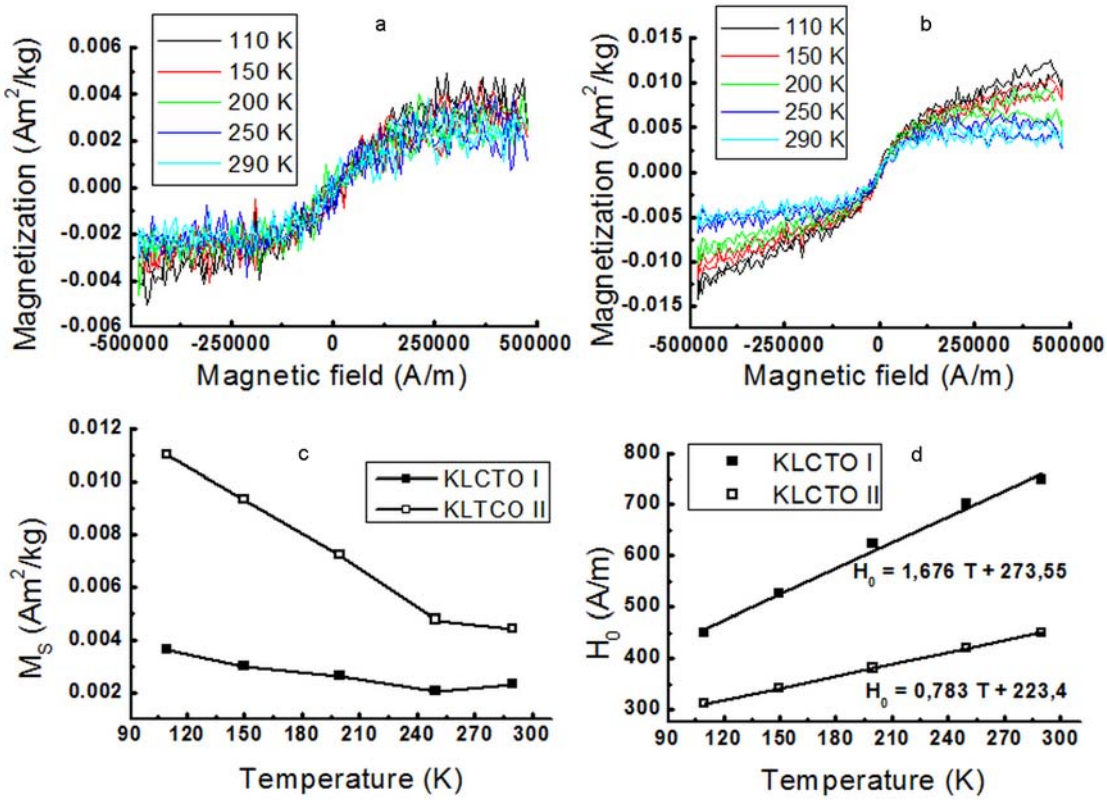

Fig.5. Magnetic hysteresis loops in the temperature range of 110–290K for KLCTO I (a) and KLCTO II (b) powder samples. Temperature dependence of saturation magnetization MS: dots are experimental data, solid lines are drawn for clarity (c); temperature dependence of H0 (d).

$4 \cdot 10^{13}$ Hz. Therefore, the co-doping with Li and Co does not affect the relaxation dynamics of Co atoms.

From experimental magnetic hysteresis loops shown in Fig. 5a, b, the saturation magnetization M_S for KLCTO I and KLCTO II samples at the investigated temperatures was obtained. Data for M_S are presented in Fig. 5c.

The non-linear shape of the magnetic hysteresis loops with an extremely small coercive field indicates the realization of a superparamagnetic state. This state is caused by magnetic nanoclusters. Inside an individual cluster, the exchange interaction between spins of Co atoms leads to their correlation, and a superspin appears, which carries a certain magnetization. In this case, long-range magnetic order is not formed due to the low concentration of the magnetic dopant. The criteria for the formation of short-range order or the conditions of magnetic percolation, such as the critical concentration of magnetic atoms and the distance between them, are discussed in [20]. This state is also called cluster ferromagnetism. Since cluster magnetism presupposes the presence of clusters of different sizes, individual clusters are correspondingly destroyed (i.e., disordered, passing from the ferromagnetic to the paramagnetic state) at different temperatures.

The analysis of magnetic hysteresis loops was performed according to the Langevin dependence [27]:

$$M = N_c M_C \left[\operatorname{cotanh}\left(\frac{M_C(H \pm H_c)}{k_B T} \right) - \frac{k_B T}{M_C(H - H_c)} \right] = M_S \left[\operatorname{cotanh}\left(\frac{H \pm H_c}{H_0} \right) - \frac{H_0}{H - H_c} \right], \quad (12)$$

where M_C is the saturation magnetization of an individual cluster, H_c is the coercive field, N_C is the number of clusters, k_B is the Boltzmann constant, M_S is the saturation magnetization of the sample, H_0 is the field at which the saturation of an individual cluster occurs. The value of H_0 is determined as follows [27]:

$$H_0 = \frac{k_B T}{M_C}. \quad (13)$$

Table 3. Parameters obtained from experimental magnetic hysteresis loops

T, K	KLCTO I			KLCTO II		
	H_0, A/m	n	$n^{1/3}$	H_0, A/m	n	$n^{1/3}$
110	450	2115	13	310	3071	14.5
150	524	2477	13.5	340	3818	15.6
200	622	2783	14	380	4555	16.5
250	700	3091	14.5	420	5151	17
290	747	3360	15	450	5577	17.7

$n^{1/3}$ is the number of cobalt atoms by the linear size of the cluster.

Accounting that $M_C = n\mu_{Co}$ and $\mu_{Co} = 1.72\mu_B$, the average number of cobalt atoms in one cluster was calculated as:

$$n = \frac{k_B T}{H_0 \mu_{Co}}. \quad (14)$$

The calculated values are shown in Table 3. The obtained temperature dependences of H_0 are shown in Fig. 5d. As seen from Fig. 5c, the saturation magnetization M_S for KLCTO I is lower than for KLCTO II in the investigated temperature range. At this, the M_S value for KLCTO I changes very slowly, from 0.011 Am^2/kg at 110 K to 0.0023 Am^2/kg at 290 K. The M_S value for KLCTO II changes twice faster, from 0.0036 Am^2/kg at 110 K to 0.0044 Am^2/kg at 290 K.

Interestingly, as the temperature rises from 110 K to 290 K, the average size of an individual cluster increases from 2115 to 3360 and from 3071 to 5577 Co atoms per cluster for KLCTO I and KLCTO II samples, respectively. An increase in the average cluster size with increasing temperature is due to the fact that smaller clusters are more sensitive to heating; therefore, they are easily disordered (destroyed). As the temperature increases, small clusters disappear, while large ones, which require more energy to destroy, remain. This leads to an increase in the average cluster size and a decrease in the saturation magnetization of the entire sample.

4. Conclusions

The effect of particle size on dielectric and magnetic properties of potassium tantalate co-doped with 4 mol.% of lithium and 4 mol.% of cobalt was investigated on powders synthesized using two different technologies: the solid-phase synthesis (KLCTO I) and the oxidation of metallic tantalum (KLCTO II). Also, undoped potassium tanthalate (KTO) was obtained by the solid-phase synthesis. From SEM data, the average particle size is 120 nm, 200 nm and 80 nm for KTO, KLTCO I and KLTCO II, respectively.

Particles of KTO and KLTCO I have a cubic shape with rounded corners, while KLTCO II has the shape of elongated formations with a longitudinal size much larger than the transverse one and clear and even edges. The elongated shape of the powder particles changes to a symmetrical cubic shape in ceramics.

The low-temperature dependence of the dielectric constant for KLCTO I is described by the Vogel-Fulcher formula with parameters $E_a = 0.0167$ eV, $T_{VF} = 22$ K and $\nu_0 = 10^7$ Hz, which characterizes the relaxation behavior of polar nanoclusters formed by off-central lithium atoms. The parameters ν_0 and E_a are found to be significantly less for KTO co-doped with lithium and cobalt in comparison with KTO doped only with lithium. The kinetic parameters describing the relaxation dynamics of Co atoms were determined from the $\tan\delta(T)$ dependences: activation energy $E_a = 0.387\pm0.05$ eV and $E_a = 0.391\pm0.05$ eV, characteristic frequency $\nu_0 = (2.5\pm0.8)\cdot10^{13}$ Hz and $\nu_0 = (3\pm1)\cdot10^{13}$ Hz for KLCTO I and KLCTO II, respectively. Therefore, a decrease in the particle size of the powder from 200 nm to 80 nm has little effect on the dynamics of cobalt.

The shape of the magnetic hysteresis loops indicates the formation of cluster magnetism with the presence of nanoclusters of different sizes in doped samples. It was found that the saturation magnetization and, accordingly, the average cluster size in the sample KLCTO I is twice smaller than in the sample KLCTO II. Therefore, in 80 nm powders (sample KLCTO I), it is easier for cobalt atoms to form larger ferromagnetic clusters than in 200 nm powders (sample KLCTO II). Analysis of the temperature dependence of the magnetic prop-

erties showed that, irrespective of the particle size, smaller clusters are easily disordered upon heating, while large ones, which require more energy to destroy, remain. As a result, the average cluster size increases, while the saturation magnetization of the entire sample decreases.

References

1. E.A.Eliseev, A.N.Morozovska, M.D.Glinchuk, R.Blinc, *J.Appl.Phys.*, **109**, 094105 (2011).
2. A.N.Morozovska, M.D.Glinchuk, E.A.Eliseev, *Phys.Rev.*, **B 76**, 014102 (2007).
3. I.S.Golovina, I.N.Geifman, Ye.V.Rodionov, Dielectric Resonators for EPR Spectroscopy. Institute of Semiconductor Physics of NAS of Ukraine, Kiev (2015).
4. I.N.Geifman, I.S.Golovina, *J.Magn.Reson.*, **74**, 292 (2005).
5. I.N.Geifman, I.S.Golovina, *Ferroelectrics*, **333**, 89 (2006).
6. I.N.Geifman, I.S.Golovina, V.I.Kofman, E.R.Zusmanov, *Ferroelectrics*, **234**, 81 (1999).
7. I.N.Geifman, I.S.Golovina, E.R.Zusmanov, V.I.Kofman, *Tech.Phys.*, **45**, 263 (2000).
8. I.S.Golovina, S.P.Kolesnik, I.N.Geifman, A.A.Andriiko, *Ferroelectrics*, **416**, 133 (2011).
9. I.S.Golovina, I.N.Geifman, N.M.Prokopiv, *Ukr.J.Phys.*, **57**, 61 (2012).
10. I.S.Golovina, S.P.Kolesnik, V.Bryksa et al., *Physica B*, **407**, 614 (2012).
11. A.N.Morozovska, E.A.Eliseev, M.D.Glinchuk, R.Blinc, *Physica B*, **406**, 1673 (2011).
12. J.J.van der Klink, F.Borsa, *Phys.Rev.B*, **30**, 52 (1984).
13. S.A.Prosandeev, E.Cockayne, B.P.Burton, *Phys.Rev.B*, **68**, 014120 (2003).
14. I.N.Geifman, I.S.Golovina, *Crystallogr.Rep.*, **39**, 57 (1994).
15. U.T.Hochli, K.Knorr, A.Loidl, *Adv.Phys.*, **39**, 405 (1990).
16. G.A.Samara, *J.Condens.Matter Phys.*, **15**, R367 (2003).
17. I.N.Geifman, A.A.Sytikov, V.I.Kolomytsev, K.Krulikovski, *Zh. Exper. Teor. Fiziki*, **53**, 1212 (1981).
18. I.N.Geifman, S.V.Svechnikov, I.A.Samoylova et al., *Fizika Tverdogo Tela*, **30**, 2824 (1988).
19. S.R.Andrews, *J.Phys.C*, **18**, 1357 (1985).
20. I.S.Golovina, S.V.Lemishko, A.N.Morozovska, *Nanoscale Res.Lett.*, **12**, 382 (2017).
21. J.S.Lee, Z.G.Khim, Y.D.Park et al., *Solid State Electron.Lett.*, **47**, 2225 (2003).
22. O.O.Andriiko, I.V.Kovalenko, L.V.Chernenko et al., *Res. Bull. NTUU "Kyiv Polytechnic Institute"*, No.1, 117 (2008).
23. H.Yokota, A.Okada, I.Ishida, L.Yoshiaki, *Jpn. J.Appl.Phys.*, **46**, 7167 (2007).
24. A.S.Nowick, S.Q.Fu, W.-K.Lee et al., *Mater.Sci.Eng.B*, **23**, 19 (1994).
25. Yu.M.Poplavko, Physics of Dielectrics. Vyshcha Shkola, Kiev (1980).
26. I.N.Geifman, I.S.Golovina, I.V.Kozlova, *Phys. Solid State*, **39**, 766 (1997).
27. S.V.Vonsovskiy, Magnetism, Nauka, Moscow (1971) [in Russian].